Neurobiology of Disease 124 (2019) 531–543

Contents lists available at ScienceDirect

Neurobiology of Disease

journal homepage: www.elsevier.com/locate/ynbdi

Human and rodent temporal lobe epilepsy is characterized by changes in O-GlcNAc homeostasis that can be reversed to dampen epileptiform activity

Richard G. Sánchez[a], R. Ryley Parrish[b], Megan Rich[a], William M. Webb[a], Roxanne M. Lockhart[a], Kazuhito Nakao[a], Lara Ianov[c], Susan C. Buckingham[a], Devin R. Broadwater[d], Alistair Jenkins[e], Nihal C. de Lanerolle[f], Mark Cunningham[b], Tore Eid[f], Kristen Riley[g], Farah D. Lubin[a,*]

[a] Department of Neurobiology, University of Alabama, Birmingham, AL, United States
[b] Institute of Neuroscience, Newcastle University, Newcastle upon Tyne, UK
[c] Civitan International Research Center, University of Alabama, Birmingham, AL, United States
[d] School of Medicine, University of Alabama, Birmingham, AL, United States
[e] Department of Neurosurgery, Royal Victoria Infirmary, Newcastle upon Tyne NE1 4LP, UK
[f] Department of Laboratory Medicine and of Neurosurgery, Yale School of Medicine, New Haven, CT, United States
[g] Department of Neurosurgery, University of Alabama, Birmingham, AL, United States

ARTICLE INFO

Keywords:
Hippocampus
Magnetic resonance imaging
Thiamet-G
Electroencephalogram
Electrophysiology
Mass spectrometry
Post-translational modification
O-GlcNAcylation

ABSTRACT

Temporal Lobe Epilepsy (TLE) is frequently associated with changes in protein composition and post-translational modifications (PTM) that exacerbate the disorder. O-linked-β-*N*-acetyl glucosamine (O-GlcNAc) is a PTM occurring at serine/threonine residues that is derived from and closely associated with metabolic substrates. The enzymes O-GlcNActransferase (OGT) and O-GlcNAcase (OGA) mediate the addition and removal, respectively, of the O-GlcNAc modification. The goal of this study was to characterize OGT/OGA and protein O-GlcNAcylation in the epileptic hippocampus and to determine and whether direct manipulation of these proteins and PTM's alter epileptiform activity. We observed reduced global and protein specific O-GlcNAcylation and OGT expression in the kainate rat model of TLE and in human TLE hippocampal tissue. Inhibiting OGA with Thiamet-G elevated protein O-GlcNAcylation, and decreased both seizure duration and epileptic spike events, suggesting that OGA may be a therapeutic target for seizure control. These findings suggest that loss of O-GlcNAc homeostasis in the kainate model and in human TLE can be reversed via targeting of O-GlcNAc related pathways.

1. Introduction

Temporal lobe epilepsy (TLE) is a neurological disorder characterized by recurrent, unprovoked seizures. Previous studies in TLE have revealed changes in cytoskeleton modifications, synaptic proteins, mitochondrial proteins, ion channels, and chaperone proteins (Liu et al., 2008; Meriaux et al., 2014). Although proteomic studies have investigated the role of post-translational modifications (PTM) in these proteins, these studies have focused mainly on phosphorylation. Protein expression and function is a dynamic process that requires precise regulation in order to maintain cellular homeostasis under changing conditions. A cellular mechanism by which cells regulate these parameters is through PTM's, where enzymes add functional groups to modulate protein dynamics. In TLE, several of these modifications are disrupted, with the majority of studies to date revealing irregularities in the extent of protein phosphorylation and its downstream effects on neuronal homeostasis (Gass et al., 1993; Mielke et al., 1999; Nateri et al., 2007; Lubin et al., 2005). Similar to phosphorylation, O-GlcNAcylation, has recently gained attention for its role in neuronal excitability in acute brain slices from non-epileptic animals (Stewart et al., 2017; Khidekel et al., 2007). Whether O-GlcNAcylation plays a role in the regulation of chronic epileptic seizures and is involvement in

Abbreviations: O-GlcNAc, O-linked-β-*N*-acetyl glucosamine; TLE, Temporal Lobe Epilepsy; PTM, post-translational modifications; OGT, O-GlcNAc Transferase; OGA, O-GlcNAcase; LTD, long-term depression; KA, kainic acid; CA, cornu ammonis; DG, Dentate Gyrus; siRNA, small interfering RNA; fEPSP, field excitatory postsynaptic potential; EPSP, excitatory postsynaptic potential; HPLC, High performance liquid chomrotagraphy; EEG, electroencephalograph; SE, Status Epilepticus; MRI, Magnetic Resonance Imaging; SORL1, Sortilin-Related Receptor; Tmod2, tropomodulin 2; LDL, low density lipid; RAP, receptor-associated protein; APP, amyloid precursor protein; AED, Anti-epileptic drugs; IP, intraperitoneal; ACSF, artificial cerebral spinal fluid; GO, Gene ontology; CSF, cerebral spinal fluid; PMI, Postmortem Interval; ABC, Alabama Brain Collection

* Corresponding author.
E-mail address: flubin@uab.edu (F.D. Lubin).

https://doi.org/10.1016/j.nbd.2019.01.001
Received 22 August 2018; Received in revised form 26 November 2018; Accepted 1 January 2019
Available online 06 January 2019
0969-9961/

protein regulation remains unknown.

O-GlcNAcylation depends on cellular metabolism in order to synthesize the substrate, UDP-GlcNAc, which is then used by O-GlcNAc Transferase (OGT) to add O-GlcNAc to serine and threonine residues (Zachara & Hart, 2006; Hart et al., 2011; Bond & Hanover, 2015). The removal of this modification is regulated by O-GlcNAcase (OGA) (Zachara & Hart, 2006; Hart et al., 2011; Bond & Hanover, 2015). Together, OGT and OGA regulate global levels of O-GlcNAcylation across a variety of cellular stresses in order to preserve homeostasis (Zachara et al., 2004). Unlike phosphorylation, in which numerous kinases and phosphatases target many of the same proteins, O-GlcNAcylation relies on only OGT and OGA (Copeland et al., 2013). Importantly, OGA can be potently and selectively inhibited by Thiamet-G, a purine analog that can cross the blood-brain barrier (Yuzwa et al., 2008). By inhibiting OGA, Thiamet-G increases global O-GlcNAcylation levels within eukaryotic cells (Yuzwa et al., 2008). Recently, several studies have focused on O-GlcNAcylation in neurological disorders such as Alzheimer's, Parkinson's, Huntington's, and other nervous system processes such as appetite, long-term depression (LTD), neuronal hyperexcitability and protein structure (Gatta et al., 2016; Wani et al., 2017a; Xie et al., 2016; Yuzwa et al., 2014; Cole & Hart, 2001; Lagerlof et al., 2016; Taylor et al., 2014; Cheung & Hart, 2008; Pekkurnaz et al., 2014; Lagerlof et al., 2017). Prior work has demonstrated that altering O-GlcNAcylation can have a therapeutic effect on acutely induced seizure activity from non-epileptic animals but it remains unknown if alterations in O-GlcNAcylation are associated with epilepsy (Stewart et al., 2017; Khidekel et al., 2007). Our current study focuses on this dynamic modification in chronically seizing epileptic animals that produce and sustain their own spontaneous seizures and are modeled more closely to human TLE. In addition to being able to observe these modifications in epileptic rodent models we were able to study these affects on ex vivo resected human TLE samples.

In the present study, we investigated the role of O-GlcNAcylation using a rodent model of TLE as well as human epileptic brain tissue, asking whether targeted manipulation of this modification could ameliorate epileptiform activity. We identified global decreases in O-GlcNAcylation in epileptic rats and in human patients with TLE. Mass spectrometry analysis revealed that O-GlcNAcylation marks were dysregulated and expressed on specific proteins in the rat epileptic hippocampus compared to age-matched non-epileptic controls. Additional experiments revealed that inhibition of OGA using Thiamet-G resulted in reduced seizure duration and decreased interictal spike frequency. Similarly, ex vivo electrophysiological recordings from human TLE samples showed decreased interictal spike activity with OGA inhibition compared to recordings taken in vehicle-treated controls. Collectively, these results support a critical role for protein O-GlcNAcylation in epilepsy and its novel therapeutic potential in the treatment of chronic seizures.

2. Material and methods

2.1. Antibodies

The following antibodies were used: 1:500 anti-O-GlcNAc (CTD110.6, MMS-248R from Covance, Princeton, NJ, USA), 1:500 anti-O-GlcNAc Transferase (O6264, Sigma, St. Louis, MO, USA), 1:20000 goat-anti-mouse (926-32,350, Licor, Lincoln, NE, USA), 1:20000 goat-anti-rabbit (926-32,211, Licor), 1:1000 anti-Actin (ab1801, Abcam, Cambridge, UK), 1:1000 anti-NeuN (MAB377, Abcam), 1:1000 anti-GFAP (ab7260, Abcam).

2.2. Kainate treatment

Animals were injected with kainic acid (KA) [10 mg/kg; (Tocris Cookson Inc., Ellisville, MO, USA)] or saline (vehicle) intraperitoneally (IP). The severity of behavioral seizures following KA injection was scored according to the Racine scale (Racine, 1972): a five-point scale which takes the five following behaviors as indicative of respectively increasing seizure severity: mouth and face clonus and head nodding (1); clonic jerks of one forelimb (2); bilateral forelimb clonus (3); forelimb clonus and rearing (4); forelimb clonus with rearing and falling (5). The onset of status epilepticus (SE) was defined as the time from KA injection to the occurrence of continuous seizure activity (Racine score 4–5) over a period of 4 h. All control animals were handled in the same manner as the KA-treated animals but injected with saline. For tissue collection, the hippocampus was removed and oxygenated (95%/5% O2/CO2) in ice-cold cutting solution (110 mM sucrose, 60 mM NaCl, 3 mM KCl, 1.25 mM NaH2PO4, 28 mM NaHCO3, 0.5 mM CaCl2, 7 mM MgCl2, 5 mM glucose, 0.6 mM ascorbate). The *cornu ammonis* (all CA regions), and the dentate gyrus (DG) region were microdissected and frozen immediately on dry ice. The hippocampus was bisected with the dorsomedial half being divided into four pieces. Using anatomic landmarks, each piece was dissected into CA and DG region. The CA and DG were dissected with a cut along the hippocampal fissure. The tissue was then stored at −80 °C for RNA and DNA extraction.

2.3. Electroencephalogram (EEG)

4 weeks following the administration of kainic acid, rats underwent an electrode implantation. Electrodes (MS333/1-B/SPC, Plastics One, Raonoke, VA, USA) for EEG recordings were trimmed to 1.75 mm in length and fitted into three holes so that they contacted the dura and the connector was flush with the skull. The ground wire was placed into the most caudal hole. For EEG recordings, animals were transferred to individual housing in custom-designed and constructed Plexiglas cages at 5 weeks. EEG data were acquired using 8 Biopac Systems amplifiers and AcqKnowlege 4.1 EEG Acquisition and Reader Software (BIOPAC Systems, Inc., Goleta, CA, USA). Data were stored and analyzed in digital format. Each cage was also equipped with an IR Digital Color CCD camera (Lorex Technology, Inc., Linthicum, MD, USA) and animals are recorded concurrently with EEG monitoring. Baseline recordings were assessed for 24 h then 10 mg/kg of Thiamet-G dissolved in 0.1% *w/v* saline (SD Chemmolecules, Owings Mills, MD, USA) was administered intraperitoneal (I·P) and then 10 mg/kg after each post-injection. Both saline and kainic acid, cohorts were injected with Thiamet-G. After 24 h of EEG recording post-injection, a second treatment with the same dosage was administered. Animals were recorded via EEG for 24 h after each injection of Thiamet-G. Animals received a total of three independent treatments at same dosage of the drug.

Tissue for Western blots was collected from 4 weeks of age using the previously-described methods. The whole hippocampus was collected and then sub-dissected. All EEG data were analyzed manually using Matlab by an observer blinded to the sample's identity. Abnormalities in the recordings indicative of epileptic activity are aligned chronologically with the corresponding video in order to confirm seizures.

2.4. Immunofluorescence

Animals were sacrificed by rapid decapitation; brains were removed, and fixed in 4% paraformaldehyde overnight at 4 °C. The next day the samples were washed with 1× PBS 5× five minutes each time before incubating with 30% sucrose (*w/v*) overnight at 4 °C. The tissue was then flash frozen on dry ice and mounted in O.C.T. (VWR, Randor, PA, USA) 10-μm Sections (10 μM) were taken throughout the dorsal hippocampus and mounted onto slides. Antigen retrieval was achieved by boiling in citric acid buffer followed by washing in 1× PBS. Slices were then blocked for 1 h (4% normal goat serum, 4% normal donkey serum and 0.3% Triton-X in PBS) and incubated in primary antibody for O-GlcNAc (1:200 CTD110.6, MMS-248R, Covance), and NeuN (1:1000, MAB377, Millipore), overnight at 4 °C. The following day sections were rinsed with 1× PBS and incubated in Alexa Fluor 488-labeled (1:500,

#111-545-003, Jackson Immuno Research, West Grove, PA, USA) or Rhodamine-labeled (TRITC, 1:500, #715-025-150, Jackson Immuno Research) secondary antibodies for 2 h and, rinsed with 1 × PBS and then cover slipped with Vectashield mounting media with DAPI (H-1500, Vector Laboratories, Burlingame, CA, USA). Images were taken on a Zeiss Axio Imager microscope and analyzed using Image J.

2.5. Human tissue samples

Pharmacologically-resistant hippocampal and cortical tissue samples from human TLE patients were provided by Tore Eid, MD from the Departments of Laboratory Medicine and of Neurosurgery, at Yale School of Medicine. Additional tissue was provided by Kristen O. Riley, MD from the Department of Neurosurgery and Yancy G. Gillespie, MD from the Wallace Tumor Institute at UAB. Acquisition and processing of control human tissue were performed by the Alabama Brain Collection (ABC) https://www.uab.edu/medicine/psychiatry/research/resources-0/alabama-brain-collection. There was no correlation between post-mortem interval (PMI) and protein levels from the ABC samples based on a Pearson's correlation (Ferrer et al., 2007; McCullumsmith et al., 2014). Patient demographics and pharmacological history are described in Supplementary Table 2.

2.6. Small animal magnetic resonance imaging

T_1- and T_2-weighted images were collected on a 9.4 T Bruker BioSpin horizontal small bore animal MRI scanner. The imaging parameters were set as follows: 1 mm slice thickness, 1 mm between slice distance, 0.1 × 0.1 × 1 mm voxel size, 30 × 30 mm FOV, 27 images per acquisition. T_2-weighted hippocampal intensities were normalized to within-slice cortical intensity using ImageJ software (n = 5/group).

2.7. Western blotting

Protein concentrations were estimated by Bradford Assay (Biorad), and 25 μg of total protein/sample was reduced in 5× sample loading buffer (0.1 M Tris-HCl, 4% SDS, 20% glycerol, 0.2% β-mercaptoethanol, 0.2% bromphenol blue), boiled for 10 min, separated by 10% SDS-PAGE, and transferred onto PVDF membranes using Trans-Blot Turbo transfer system (1,704,155, BioRad, Hercules, CA, USA). Membranes were activated with methanol for three minutes before transfer, blocked for 1 h at room temperature and incubated overnight at 4 °C with primary antibodies following the transfer. Three washes were performed with 1× PBST (PBS and 0.01% Tween) between primary and secondary antibodies and after stripping. The membranes were blocked with 1:1 Licor Blocking buffer (P/N 927-40,003, Licor) and PBST for one hour at room temperature after transfers and stripping. Imaging was performed using Licor Odyssey scanner at 700/800 channel, and Licor Odyssey software. Image analysis was performed using Image Studio Lite Ver. 3.1.

2.8. Sample preparation for mass spectrometry

Protein was extracted from rat dorsal hippocampus CA using M-PER (78,501, Thermo Fisher Scientific) and quantified using Pierce BCA Protein Assay Kit (23,225, Thermo Fisher Scientific). Extracts were diluted in LDS PAGE buffer (NP0007, Invitrogen) followed by reduction, heat denaturing, and separation on an SDS Bis-Tris gel (4–12%, NP0323BOX, Invitrogen). The gels were stained overnight with colloidal blue (89,871, Invitrogen). The entire lane comprising each sample was cut into 12 MW fractions and equilibrated in 100 mM ammonium bicarbonate (AmBc). Gel slices were reduced, carboxymethylated, dehydrated, and digested with Trypsin Gold (V5280, Promega, Madison, WI, USA) as per manufacturers' instructions. Following digestion, peptides were extracted, the volume was then be reduced in a SpeedVac to near dryness, and resuspended to 20μl using 95% ddH_2O/ 5% ACN/ 0.1% formic acid (FA) prior to analysis by 1D reverse phase LC-ESI-MS2 (as outlined below).

2.9. HPLC-electrospray tandem mass spectrometry

Peptide digests were injected onto a 1260 Infinity HPLC stack (Agilent, Santa Clara, CA, USA) and separated using a 75 μm I.D. x 15 cm pulled tip C-18 column (00G-4053-E0, Jupiter C-18300 Å, 5 μm, Phenomenex, Torrance, CA, USA). This system runs in-line with a Thermo Orbitrap Velos Pro hybrid mass spectrometer, equipped with a nano-electrospray source (Thermo Fisher Scientific), and all data was collected in CID mode. The HPLC was configured with binary mobile phases that include solvent A (0.1%FA in ddH_2O), and solvent B (0.1% FA in 15% ddH_2O / 85% ACN), programmed as follows; 10 min @ 0%B (2 μL/ min, load), 120 min @ 0%-40%B (0.5 nL/ min, analyze), 15 min @ 0%B (2 μL/ min, equilibrate). Following each parent ion scan (350-1200 m/z @60 k resolution), fragmentation data (MS2) was collected on the topmost intense 15 ions. For data dependent scans, charge state screening and dynamic exclusion were enabled with a repeat count of 2, repeat duration of 15.0 s, and exclusion duration of 60.0 s.

2.10. Mass spectrometry data conversion and searches

The XCalibur RAW files were collected in profile mode, centroided and converted to MXML using ReAdW v. 3.5.1. The mgf files were then created using MzXML2Search (included in TPP v. 3.5) for all scans. The data was searched using SEQUEST, which was set for two maximum missed cleavages, a precursor mass window of 20 ppm, trypsin digestion, variable modification C at 57.0293, and M at 15.9949. Searches were performed with a species-specific subset of the UniRef100 database.

2.11. Peptide filtering, grouping, and quantification

The list of peptide IDs generated based on SEQUEST search results were filtered using Scaffold (Protein Sciences, Portland, OR, USA). Scaffold filters and groups all peptides to generate and retain only high confidence IDs while also generating normalized spectral counts (N-SC's) across all samples for the purpose of relative quantification. The filter cut-off values were set with minimum peptide length of > 5 AA's, with no MH + 1 charge states, with peptide probabilities of > 80% C.I., and with the number of peptides per protein ≥2. The protein probabilities are then set to a > 99.0% C.I., and an FDR < 1.0. Scaffold incorporates the two most common methods for statistical validation of large proteome datasets, the false discovery rate (FDR) and protein probability (Weatherly et al., 2005; Keller et al., 2002; Hensley et al., 1995). Relative quantification across experiments were then performed via spectral counting, and when relevant, spectral count abundances were then normalized between samples (Liu et al., 2004; Old et al., 2005; Beissbarth et al., 2004).

2.12. Proteomics analysis

For the proteomic data generated, two separate non-parametric statistical analyses were performed for each pair-wise comparison. These non-parametric analyses include 1) the calculation of weight values by significance analysis of microarray (SAM; cut off > |0.6| combined with 2) T-Test (single tail, unequal variance, cut off p < .05), which then were sorted according to the highest statistical relevance in each comparison. For SAM, whereby the weight value (W) is a statistically derived function that approaches significance as the distance between the means (μ1–μ2) for each group increases, and the SD (δ1-δ2) decreases using the formula, W = (μ1–μ2)/(δ1–δ2) (Golub et al., 1999; Xu et al., 2015). For protein abundance ratios determined with N-SC's, we set a 1.5–2.0 fold change as the threshold for significance, determined empirically by analyzing the inner-quartile data

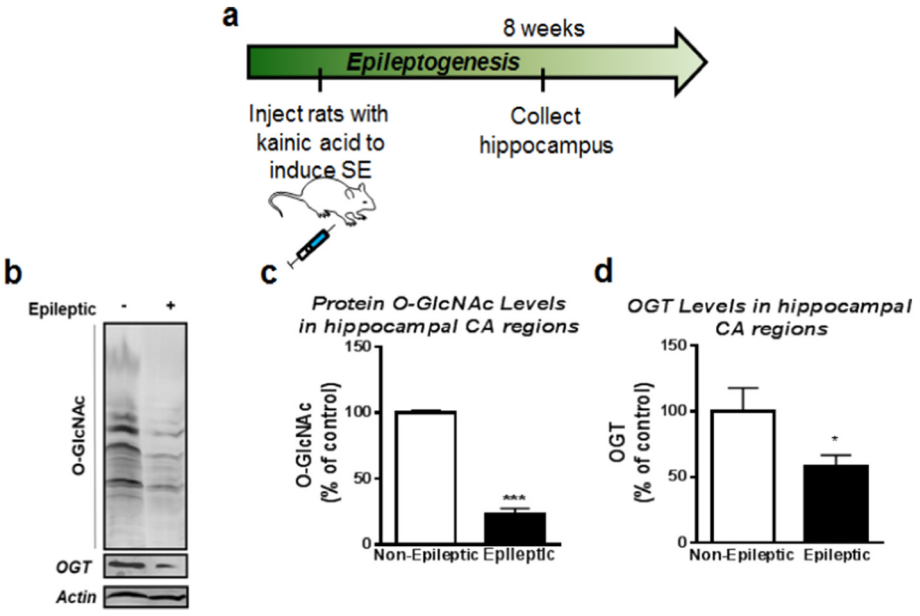

Fig. 1. O-GlcNAcylation and OGT levels decreased in the hippocampus of epileptic rats. (a) Experimental design. Rats were either injected with saline or kainic acid in order to induce status epilepticus (SE). The animals were then sacrificed eight weeks post-KA injection at which point these animals had become epileptic and the hippocampus was collected for protein analysis. (b) Representative O-GlcNAcylation as well as OGT and actin western blots for controls and epileptic rats. (c) Global O-GlcNAcylation was decreased in epileptic rats in comparison to control. (n = 4–6 per group) (d) OGT protein levels were significantly reduced in epilepsy (n = 4–6 per group).* denotes $P < .05$ from controls, *** denotes $P < .001$ from controls. Unpaired T-Test Error bars are SEM.

from the control experiment indicated above using ln-ln plots, where Pierson's correlation coefficient (R) was 0.98, and > 99% of the normalized intensities fell between ± 1.5 fold. In each case, any two of the three tests (SAM, Ttest, or fold change) had to pass.

Gene ontology assignments and pathway analysis were carried out using MetaCore (GeneGO Inc., St. Joseph, MI, USA). In addition, the final proteins list is analyzed using the auto-expand algorithm within MetaCore using the default setting (i.e. expanded by 50 nodes). In parallel, the expand-by-one algorithm is used to identify connections to the neighboring proteins, known drug interactions, and any known correlation to a disease, or specific biological process. Interactions identified within MetaCore are manually correlated using full-text articles. Detailed algorithms have been described previously (Bhatia et al., 2009; Ekins et al., 2006). The heatmap was constructed in R with the package 'ComplexHeatmap' (v 1.18.0) and the scatter plots were created with 'ggplot2' (v 2.2.1.9000).

2.13. Human electrophysiology

The electrophysiological data obtained from ex vivo slice studies were derived from patients with medically intractable epilepsy undergoing elective neurosurgical tissue resection for the removal of a sclerotic hippocampus. All patients gave their informed consent, before surgery, for the use of the resected brain tissue for scientific studies. This study was approved by the Newcastle and the North Tyneside 2 Local Research Ethics Committee (06/Q1003/51) (date of review 03/07/06) and had clinical governance approved by the Newcastle Upon Tyne Hospitals NHS Trust (CM/PB/3707). Slices were prepared from these samples using methods as previously described (Roopun et al., 2010; Cunningham et al., 2012; Simon et al., 2014). The time between resection and slice preparation was < 5 min. Extracellular recordings (DC–500 Hz) were conducted with ACSF-filled glass microelectrodes (2 MΩ) connected to an extracellular amplifier (EXT-10-2F, npi electronic GmbH, Tamm, Germany). Signals were digitized (5 kHz) and recorded on a computer and then extracellular field recordings were analyzed to detect events using a custom-written code in Matlab2015b (Mathworks, MA, USA).

2.14. siRNA infusion

For electrophysiological studies, hippocampal slices were collected from 6 to 8 week old, male Sprague-Dawley rats as previously described (Lubin et al., 2005). All rats had previously undergone stereotactic cranial infusion of siRNA according to previously described methods (Webb et al., 2017). Briefly, animals were anesthetized by way of intraperitoneal injection of dexmedetomidine-ketamine and received bilateral infusions of Accell SMARTpool siRNAs (Thermo) targeting either OGT (#E-080125-00-05) or scrambled, negative controls (#D-001910-10-05) in the dorsal hippocampus using the following stereotaxic coordinates relative to bregma: A/P -3.6 mm, M/L ± 1.7 mm, D/V -3.6 mm. Infusions were delivered at a constant rate of 0.1 uL per minute using a linear actuator for a total volume of 1 uL per side. Non-targeting, fluorescent Accell siRNA (#D-001960-01) were used to confirm targeted delivery of siRNA to the dorsal hippocampus. For all conditions, fresh stocks of siRNA (100 µM) were re-suspended in Accell siRNA resuspension buffer to a concentration of 4.5 µM immediately prior to surgery.

2.15. Electrophysiology

Following surgery, each rat was allowed five days of recovery time after which its brain was harvested and hippocampal slices were collected for further testing. High-frequency stimulation of the Schaffer collateral/commissural pathway (CA3-CA1) was conducted using four trains of 100 pulses at 100 Hz, spaced 60 s apart. The initial slope of the field excitatory postsynaptic potential (EPSP) was measured as an index of synaptic strength. Percent fEPSP slopes were averaged after 20 min of baseline recording. Electrophysiological data are reported as means ± SEM, where n represents the number of slices.

2.16. Statistical analysis for biochemistry studies

Data is expressed as mean ± S.E.M and compared by a Student-test and Mann-Whitney. Shapiro-Wilk and Kolmogorov-Smirnov statistics were performed to take into account any age, sex, race, and post-mortem interval information, none of the listed factors are contributing to our results for the OGT or O-GlcNAc protein levels for the human experiments. Statistically significant differences between groups were defined as $p < .05$.

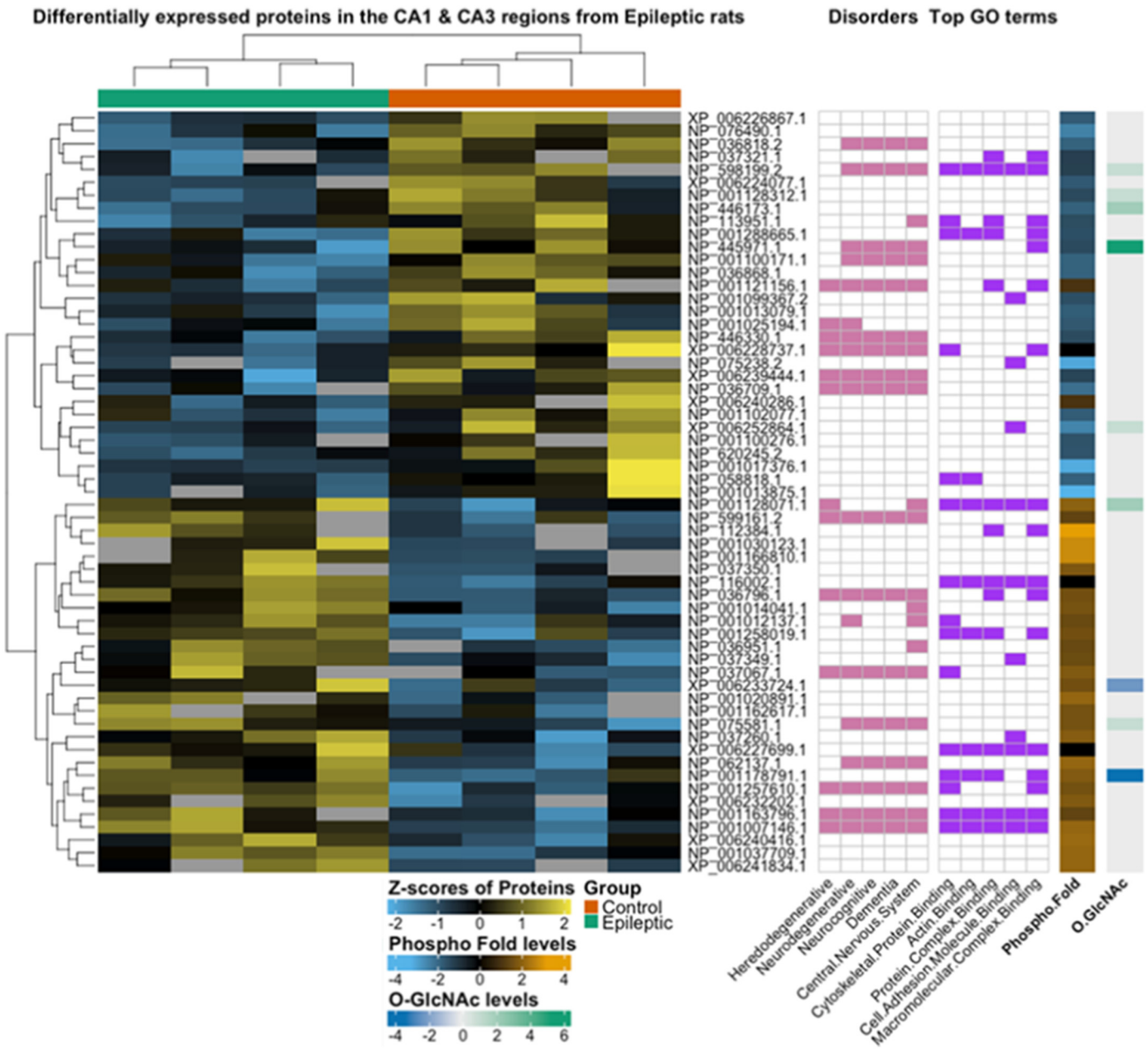

Fig. 2. Protein expression and PTM in epilepsy. (a) The heatmap illustrates all differentially expressed proteins ($p < .05$) in epileptic rats (green bar) relative to controls (orange) bar. Each row is a protein indicated by the RefSeq accession number and each column in a biological replicate where the row and column order was determined by the Euclidian clustering method shown by the dendrograms. The protein values are shown as standardized z-scores, where the color indicates the standard deviation increasing (yellow) or decreasing (blue) relative to the mean (black). Grey blocks indicate missing values for the respective biological replicate. Further, for each protein, the top five disorders and GO terms (adjusted *p*-value < .05) are annotated in pink and purple respectively. Lastly, the phosphorylation (phospho) fold change and O-GlcNAc levels are indicated for each differentially expressed protein.* denotes $P < .05$ from controls, *** denotes $P < .001$ from controls. Unpaired *T*-Test Error bars are SEM. (For interpretation of the references to color in this figure legend, the reader is referred to the web version of this article.)

3. Results

3.1. Hippocampal O-GlcNAcylation and OGT protein levels decreased in epileptic rats

KA-induced epilepsy has been shown to alter a variety of PTMs in proteins of the hippocampus. Therefore we sought to quantify global O-GlcNAcylation levels in the hippocampus eight weeks post-SE when the animals had become fully epileptic and experienced self-convulsive seizures (Fig. 1a). Analysis of protein O-GlcNAcylation in the CA regions of the hippocampus revealed significant decreases of O-GlcNAcylation in epileptic animals compared to controls ($t_{(4)} = 13.02$, $p = .0002$, $t_{(8)} = 2.363$, $p = .0457$; Fig. 1b-c). To investigate this decrease further, we measured OGT protein levels in the same region and observed a significant decreased in OGT protein levels in the epileptic rats when compared to controls($t_{(4)} = 13.02$, $p = .0002$, $t_{(8)} = 2.363$, $p = .0457$; Fig. 1d). In light of these results, we wanted to understand whether loss of OGT contributed to neuronal hyperexcitability. Following siRNA-mediated knockdown of OGT and high-frequency stimulation of the Schaffer collateral/commissural pathway in wild-type rats (Supplemental Fig. 1a-c), we detected a trend toward increasing percent fEPSP and fEPSP slope. Our findings suggest an increased rate

of neuronal firing with reduction of OGT. Meanwhile, no changes were detected in the paired-pulse facilitation between groups, indicating that any changes in neuronal firing were due to changes in the postsynaptic neuron. Taken together, these results indicate a reduction of O-GlcNAc and OGT protein levels in the epileptic hippocampus and suggest a correlation between epilepsy and protein O-GlcNAcylation.

Next, we sought to investigate specific proteins that displayed differential O-GlcNAcylation expression associated with TLE pathology. Using HPLC-electrospray tandem mass spectrometry we measured the abundance of proteins that had differentially altered O-GlcNAcylation expression in the CA regions of the hippocampus at eight weeks post-SE. We found that 59 proteins were differentially expressed in TLE. Within those 59 proteins, only 17 proteins had O-GlcNAc modifications with 9 of which that were differentially O-GlcNAcylated. Gene ontology analysis revealed that the majority of diseases associated with differential expression of these proteins were neurodegenerative or cytoskeletal in nature. Additionally, among these 17 proteins, 12 had been associated with epilepsy in previous studies (Khidekel et al., 2007) (Supplementary Table 1) (Fig. 2A).

In addition to measuring O-GlcNAcylation, we also measured phosphorylation and discovered increases in protein phosphorylation, particularly on those proteins that had shown decreases in protein O-GlcNAcylation. We next analyzed overall protein expression against protein phosphorylation and protein O-GlcNAcylation (Supplemental Fig. 2a-b) revealing two distinct cluster groups. These clusters indicated that increased protein expression was positively correlated with increased protein phosphorylation, and only a few of the more highly expressed proteins also had changes in O-GlcNAcylation. In contrast to phosphorylation, increased protein O-GlcNAcylation was predominantly present on proteins that showed decreased expression. These clusters persisted when O-GlcNAcylation and phosphorylation were plotted against each other (Supplemental Fig. 2c). The *Z*-scores were plotted from each biological replicate against either modification to demonstrate the contrast between their fold change (Supplemental Fig. 2d-e). Taken together our mass spectrometry analysis corroborated our findings that overall protein O-GlcNAcylation was decreased in the epileptic animal hippocampus while highlighting the particular proteomic ontologies affected by this loss. Additionally, our findings revealed that certain proteins actually show increased O-GlcNAcylation in the epileptic hippocampus. Collectively, these findings provide evidence that differentially expressed proteins and changes in PTMs are associated with TLE and other disease states highlighting the importance of protein PTM in homeostasis.

3.2. OGA inhibition via acute Thiamet-G treatment reduced epileptiform activity in the epileptic hippocampus

The observed global loss of O-GlcNAcylation and OGT prompted additional experiments to determine the role of this PTM in epilepsy. Using the KA model of epilepsy, we recorded brain neuronal activity with EEG one month post-SE. We then administered Thiamet-G (10 mg/kg/day), a known OGA inhibitor used to increase O-GlcNAcylation, once a day for three consecutive days in order to measure its effect on epileptiform activity (Fig. 3a). We measured baseline EEG activity between control animals and epileptic animals and found that epileptic animals demonstrated higher power than the controls indicating more epileptiform activity or the integral average of the amplitude of the EEG signal across time (Fig. 3b-c). The epileptic rats presented with more sharp spikes and larger amplitudes of voltage than the control animals, suggesting synchronous activity or seizures in the spectrogram depicted with warmer colors. The epileptic animals then underwent a daily regimen of OGA inhibition for three days while being monitored with EEG (Fig. 3d). Following three days of Thiamet-G treatment, epileptic rats displayed a reduction in epileptiform activity displaying decreases in sharp spikes and voltage amplitudes as well as a decrease in the seizure frequency and duration ($t_{(7)} = 1.999, p = .858$, $t_{(34)} = 3.497$, $p = .0013$; Fig. 3e-f). We then assessed different wave oscillations from EEG recordings in order to determine if there were any changes in band power between frequencies for each day of Thiamet-G treatment. (Fig. 3g). The frequencies were divided into the lower band frequencies, such as delta and theta waves, which are associated with sleep, and the higher frequency bands such as gamma, which is more closely associated with consciousness and attentiveness (Cahn & Polich, 2006). These bands can be used to characterize seizure severity (Fisher et al., 1992; Worrell et al., 2004; Haddad et al., 2014). In this study, OGA inhibition helped restore the power of the lower frequencies (delta-alpha) more so than the higher frequencies (beta-gamma) to the baseline of the control group.

We furthered analyzed each frequency type against their relative power. As expected the largest powers for each given frequency band were from the epileptic rat recordings prior to Thiamet-G treatment ($t_{(32–52)} =$, $p = .0016– < 0.0001$; Fig. 3h). By the first day of treatment, these bands showed a reduction in power and began to mirror the power levels of the non-epileptic rats, with the exception of the gamma frequency. The gamma frequency was the least affected by treatment; this could be explained by a local measure of activity and not by an overall global cortical network due to a single measurement of activity with an electrode. With each day of treatment, the relative power of each band decreased with the exception of the theta band which plateaued after the first treatment of Thiamet-G. The excitatory regular spiking, and pyramidal neuron intrinsic bursting typically characterize this band, suggesting that inhibition of OGA via Thiamet-G may preferentially target this group of neurons.

3.3. Chronic inhibition of OGA activity increased hippocampal atrophy in epileptic rats

Since OGA inhibition dampened epileptiform activity and seizure duration in a wide spectrum of frequencies, we sought to determine if there were any morphological changes associated with Thiamet-G treatment over a prolonged period of usage. Hippocampal scarring and/or gliosis is often observed in animal models of TLE as well as in humans, where it leads to hippocampal atrophy (Al Sufiani & Ang, 2012; Crespel et al., 2002; Engel Jr., 1996; Sofroniew & Vinters, 2010). Hippocampal atrophy in TLE patients has been observed using MRI T_2 weighted scans where the ventricles adjacent to the hippocampus expand along with a reduction of hippocampal size (Thom, 1917; Fuerst et al., 2003; Dabbs et al., 2012). We created epileptic rats as previously described, and performed T_2 weighted MRI eight weeks post KA in order to record their ventricular volumes prior to Thiamet-G treatment. We then began a two-week treatment regimen for these animals as well as non-epiletic controls with either saline or Thiamet-G (10 mg/kg/day) and measured their ventricular volumes after treatment (Fig. 4a-c One way ANOVA, $F = 10.05$, $p = .0002$). Epileptic rats displayed significantly higher voxel area units prior to treatment compared to non-epileptic controls. Following two weeks of treatment, voxel area increased in both Thiamet-G treated rats and saline-treated epileptic rats indicating no restoration of hippocampal morphology with Thiamet-G treatment.

With the most significant ventricle increases observed in Thiamet-G treated epileptic rats. These scans suggest that Thiamet-G does little to inhibit or slow the progression of ventricular expansion seen in epilepsy (Dabbs et al., 2012; Coulter & Steinhauser, 2015; Wieshmann et al., 1997; Jackson et al., 2011).

Following MRI scans, animals were sacrificed and brain tissue was processed for immunohistochemistry experiments. We stained brain slices for O-GlcNAcylation (Supplemental Fig. 3b) as an output for Thiamet-G treatment. We observed increases in O-GlcNAcylation with Thiamet-G treatment in the hippocampus particularly in the molecular layer in both control and epileptic rats that received Thiamet-G. Taken together, these experiments suggest that OGA inhibition does not stop or reverse epileptic hippocampal atrophy. These findings leave open the

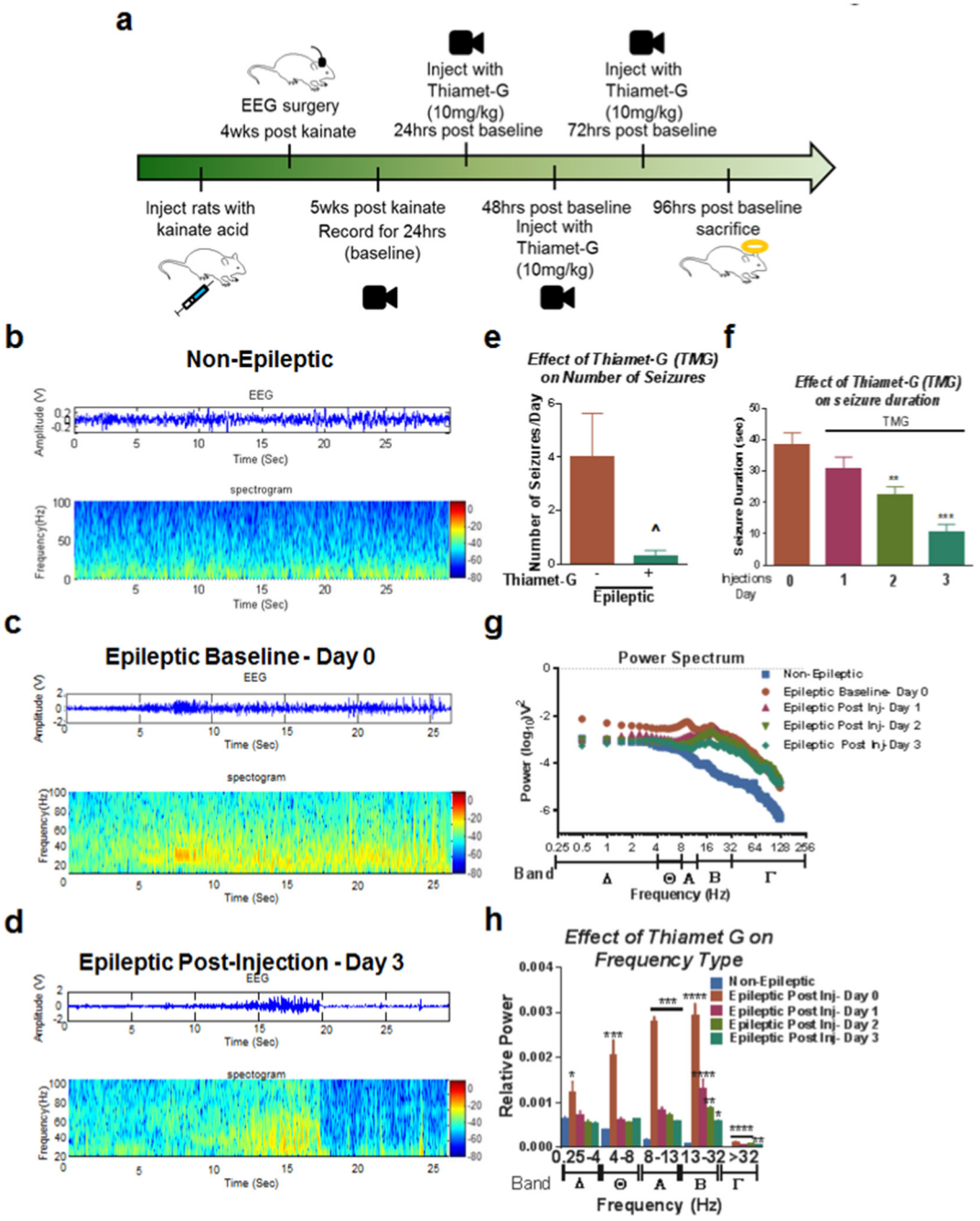

Fig. 3. OGA inhibition decreased seizure duration and epileptiform activity. (a) Experimental outline. Epileptic rats were created using kainic acid. Four weeks post kainate the rats underwent EEG surgery where cortical electrodes were placed and the animals had a week to recover from the surgery before recordings were initiated. Baseline recordings were taking for 24 h and Thiamet-G treatment ensued immediately after for three consecutive days followed by euthanization. (b) Cortical baseline EEG spectrogram of a saline (control) treated rat. (c) Cortical baseline EEG spectrogram of an epileptic rat during a seizure. (d) Cortical EEG spectrogram of the same epileptic rat following three days of Thiamet-G treatment. (e) The number of seizures decreased after three days of Thiamet-G treatment between the pre and post-treated animals. (f) Thiamet-G significantly decreased seizure duration by the second day of treatment and continued to decrease seizure duration up to the last day of treatment. (g) A power spectrum analysis demonstrated that the frequencies that were most dampened by Thiamet-G intervention were theta through gamma bands (h) Quantification of the power spectrum illustrates which frequencies were significantly decreased after treatment in comparison to control non-epileptic animals. * denotes $P < .05$ from controls, ** denotes $P < .01$ from controls, *** denotes $P < .001$ from controls, **** denotes $P < .0001$ from controls. ˆ denotes $P < .10$ One-way ANOVA, Error bars are SEM.

possibility that Thiamet-G treatment may slow the progression of hippocampal atrophy if it is begun earlier in the disorder. However, OGA inhibition at a chronic seizure state does not appear to restore atrophied tissue.

Because Thiamet-G treatment resulted in increased O-GlcNAcylation expression in epileptic animals, we next sought to understand how chronic treatment with Thiamet-G would affect O-GlcNAcylation levels on proteins shown to be O-GlcNAcylated and differentially expressed in TLE. Specifically, we wanted to ask whether OGA's expression was altered in epilepsy, and if so, whether Thiamet-G treatment restored OGA expression to homeostatic levels. We first looked at OGA protein expression in our epileptic animals that were treated for two weeks with Thiamet-G, (One way ANOVA $F = 1.852$ $p = .085$, Fig. 3d-e).We noticed no significant changes in OGA protein

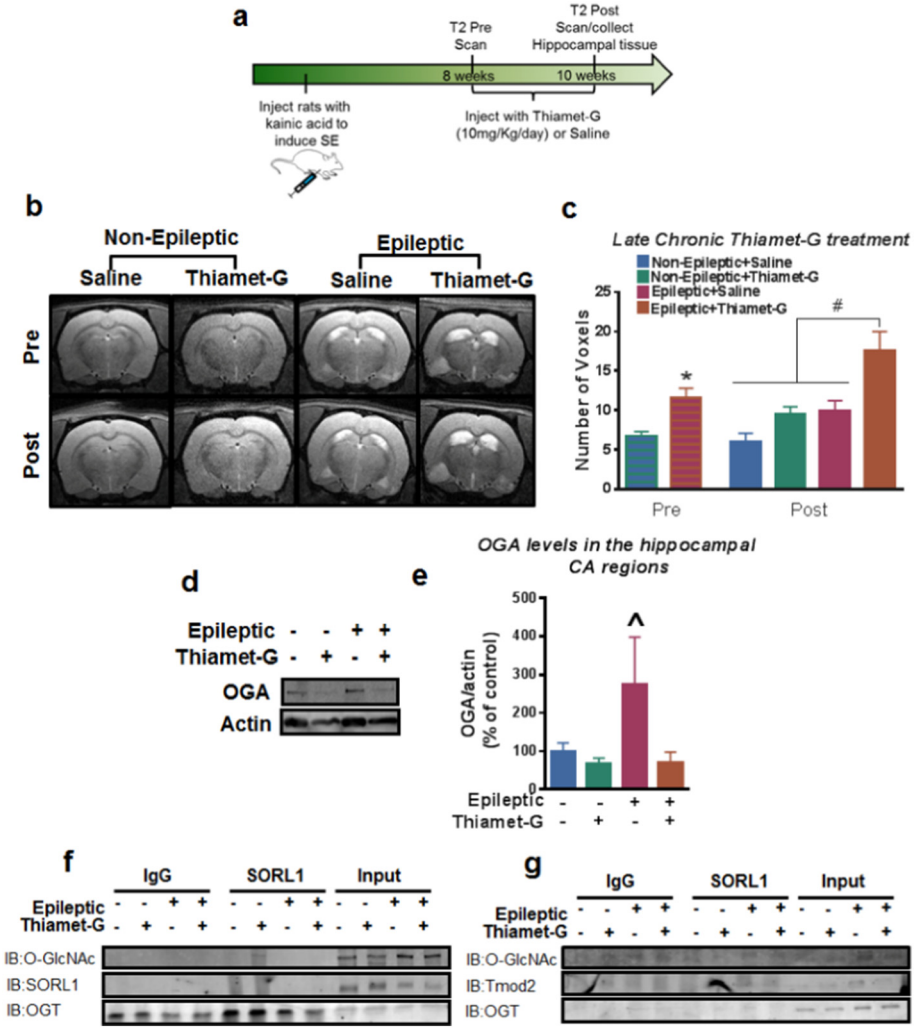

Fig. 4. Thiamet-G treatment has no reduction in ventricle expansion or protein specific changes in O-GlcNAcylation. (a) Experimental outline of animal model and treatment. Epileptic animals were created with kainic acid. Eight weeks post-kainate the animals had their first T2 scans were taken. Immediately following the scan, animals were treated with Thiamet-G (10 mg/kg/day) for 2 weeks at the same time each day. The animals then had a final T2 scan where they were then sacrificed and the hippocampus was collected. (b)Representative pre/post T2 weighted images of epileptic and non-epileptic rats that were treated with either saline or Thiamet-G for two weeks. The CSF is bright white in the T2 MRI images demonstrating ventricle expansion with epilepsy and a more severe expansion with Thiamet-G treatment. (c) Quantification of T2 MRI images showing significant ventricle sizes between controls and epileptics before Thiamet-G treatment. Ventricle sizes significantly differed between the epileptic Thiamet-G treated group and the rest of the other group's post-treatment. (n = 8/group). (d) Representative western blots of OGA and actin for the two-week saline or Thiamet-G treated epileptic and non-epileptic rats. (e) statistical analysis of the two-week saline or Thiamet-G treated epileptic and non-epileptic rats normalized to actin. (f) Immunoprecipitation of SORL1 with immunoblotting for O-GlcNAc (top membrane), SORL1 (middle membrane), and OGT (bottom membrane). (g) Immunoprecipitation of Tmod2 with immunoblotting for O-GlcNAc (top membrane), Tmod2 (middle membrane), and OGT bottom (membrane). (n = 6–7/group) * denotes $P < .05$ from Non-epileptic plus saline controls. #denotes $P < .05$ from Epileptic plus Thiamet-G. ^denotes $P < .10$ from Non-epileptic plus saline controls. One-way ANOVA. Error bars are SEM.

expression in control animals treated with Thiamet-G. Although not significant, we did notice a trend in increased OGA protein expression in epileptic animals. When these animals were treated with Thiamet-G, levels of OGA expression resembled those of saline-treated controls.

Based on our proteomic analysis (Fig. 2a), we identified Sortilin-Related Receptor (SORL1) and tropomodulin 2 (Tmod2) as proteins that undergo increased and decreased protein O-GlcNAcylation in TLE, respectively (Supplemental Fig. 4). SORL1 is a receptor that binds to LDL and transports it into the cells via endocytosis, a process that is subject to inhibition upon binding to the receptor-associated protein (RAP) (Bu, 2001). SORL1 has also been implicated in APP trafficking to and from the Golgi apparatus in Alzheimer's disease (Zollo et al., 2017; Yin et al., 2015). Tmod2 is an actin-binding protein that stabilizes ADP-bound actin monomers onto actin filaments and is downregulated in epilepsy (Yang et al., 2006; Sussman et al., 1994). To test the effect of Thiamet-G administration on these proteins' PTMs we used immunoprecipitation followed by Western blot to investigate the levels of O-GlcNAcylaion on these proteins specifically. We observed no differences in O-GlcNAcylation on immunoprecipitated SORL1, nor did we observe any difference in its association with OGT (Fig. 4f). Immunoprecipitation of Tmod2 revealed slight increases in O-GlcNAcylation in animals treated with Thiamet-G, along with decreases of total O-GlcNAcylation in the inputs, or the raw unimmunoprecipitated samples (Fig. 4g). Furthermore, no differences were observed in the degree of association between Tmod2 and OGT. These results suggest that Thiamet-G cannot restore the decreased levels of O-GlcNAcylation of SORL1 and Tmod2 specifically in epileptic rats.

3.4. Deficits in O-GlcNAcylation and OGT in patients with TLE

Our initial rodent studies have shown that O-GlcNAcylation and OGT are downregulated in the hippocampi of epileptic rats, but we were unsure of how O-GlcNAcylation and OGT might behave in human TLE tissue (Supplementary Table 2). We began by measuring O-GlcNAcylation and OGT expression in resected human hippocampus from TLE patients and compared them to age-matched controls from post-mortem human hippocampal tissue (Fig. 5a). We observed a significant loss of O-GlcNAcylation and OGT expression ($t_{(18)} = 3.198$, $p = .0050$, $t_{(11)} = 1.941$, $p = .0783$ Fig. 5b-c) in TLE patient tissue compared to control postmortem tissue as seen in our epileptic rats. We next asked whether SORL1 and Tmod2 were being modified in the same manner that we had seen in our epileptic rats. We immunoprecipitated SORL1 (Fig. 5d) and Tmod2 (Fig. 5e) from human postmortem samples and similar to our results in rodent tissue, we observed no differences in O-GlcNAcylation of the proteins, nor any differences in their interaction with OGT.

3.5. OGA inhibition decreased spike events and increased OGT and OGA protein expression in human TLE resected tissue

Because we observed decreases in O-GlcNAcylation levels in samples from human TLE patients, we next sought to test whether bath application of Thiamet-G could reduce epileptiform activity in live TLE patient tissue. As previously described (Roopun et al., 2010), baseline spontaneous interictal-like activity was recorded for 1 h, after which,

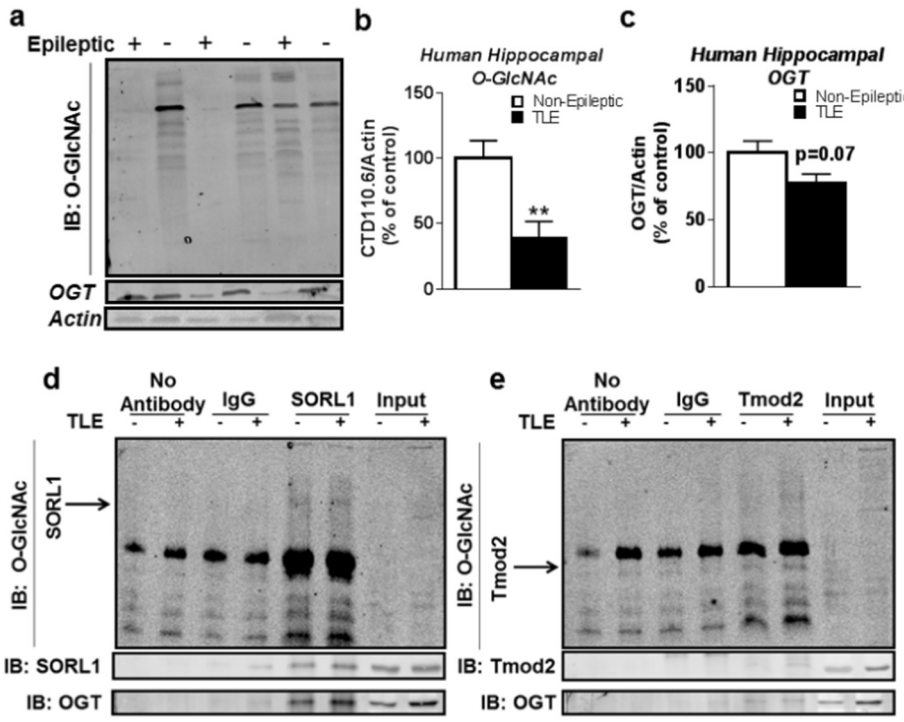

Fig. 5. Tissues from patients with TLE have significant deficits in O-GlcNAcylation and OGT (a) Western blot membrane with TLE human tissue and post-mortem non-epileptic alternating from left to right. The top membrane was probed with CTD110.6 antibody to show O-GlcNAc levels between both groups. The middle membrane was stripped and probed with OGT and the bottom membrane represents the level of actin between both groups. (b) Desensitization of O-GlcNAc levels between control and TLE individuals were quantified and actin was used to normalize O-GlcNAc. (n = 11–13 per group) (c) Desensitization of OGT levels between control and TLE where taken and normalized to actin. (n = 11–13 per group). Immunoprecipitation of (d) SORL1 and (e) Tmod2 on resected TLE patients and postmortem tissue. Immunoblotting was performed with O-GlcNAc (top membrane), SORL1 (middle membrane), Tmod2 (middle membrane), and OGT (bottom membrane). Unpaired T-Test. **denotes $P < .01$. Error bars are SEM.

slices were then exposed to Thiamet-G (100 μM) (Fig. 6a). Prior to treatment with Thiamet-G, tissue slices exhibited spontaneous interictal-like activity at an average of 66 spikes per minute (+/− 6.8 spikes/min), a rate which decreased to an average of 40 spikes per minute (+/− 8.9 spikes/min) after one hour of Thiamet-G treatment (Fig. 6b-d).

Interestingly, our human electrophysiological data revealed no immediate decreases in epileptiform activity following Thiamet-G administration indicating that it is most likely functioning through PTM of proteins altering their structure and function over time as oppose to direct interactions with ionic channels/receptors. Importantly, slices that were not treated with Thiamet-G had an average of 78 spikes per minute (+/− 4.8 spikes/min), with no change in average spikes over time, demonstrating that time cannot account for the decrease in spikes per minute observed with Thimaet-G treatment. Thus, application of Thiamet-G to spontaneous hyper-excitable human epileptic tissue significantly decreased spike frequency.

We next examined the O-GlcNAcylation, OGT, and OGA levels in these tissues (Fig. 6e). Protein O-GlcNAcylation generally increased with Thiamet-G treatment in comparison to untreated resected tissue (Fig. 6f). OGT and OGA, which is enzymatically inhibited by Thiamet-G, increased with Thiamet-G treatment. Overall, we found that O-GlcNAcylation and OGT levels decreased in epilepsy, but promoting this PTM pharmacologically resulted in decreased seizure frequency and spiking, as well as increased protein O-GlcNAcylation.

4. Discussion

The role of protein O-GlcNAcylation in the epileptic hippocampus is yet to be determined. The current study demonstrates that O-GlcNAcylation and OGT is decreased in the hippocampus from a rodent model of epilepsy, and in resected human TLE tissue. Using the OGA inhibitor Thiamet-G, we were able to increase bulk protein O-GlcNAcylation levels, not only in the rodent epileptic hippocampus, but in resected human hippocampal TLE tissue as well. Pharmacologically increasing bulk protein O-GlcNAcylation levels led to reduced seizures and epileptiform activity in in the rodent epileptic hippocampus and in resected tissue from human TLE patients. Together, these results suggest that an imbalance in protein O-GlcNAcylation in the epileptic hippocampus can be reversed to lessen seizure episodes. Moreover, we demonstrate that the highly selective OGA inhibitor Thiamet-G can cross the blood-brain barrier to promote protein O-GlcNAcylation in the hippocampus, which provides a potentially novel and viable therapeutic option for epilepsy treatment.

Our finding of promoting protein O-GlcNAcylation decreases epileptiform activity is further supported by prior studies investigating O-GlcNAcylation in non-epileptic seizure models suggesting that this PTM may be involved in the maintenance of seizure activity (Stewart et al., 2017; Khidekel et al., 2007). For example, with the epileptic KA model, O-GlcNAcylation levels, initially increased and subsequently decreased several hours post-SE (Khidekel et al., 2007). Alternatively, pentylenetetrazol (PTZ) induction of non-epileptic seizures produced no changes in bulk O-GlcNAcylation levels, yet treatment with Thiamet-G decreased epileptiform activity following PTZ induced seizures (Stewart et al., 2017). Collectively, these prior studies demonstrate differential regulation of the O-GlcNAc axis in non-epileptic seizures compared to epileptic seizures, indicating that epileptogenesis and etiology of seizures with respects to the O-GlcNAc axis is worth noting. Thus, our current study expands on these prior findings by providing insight into the proteomic manner in which protein O-GlcNAcylation affects the epileptic hippocampus. Moreover, we provide evidence that O-GlcNAcylation protein may diminish seizures and epileptiform activity by targeting this modification to specific proteins altered in epilepsy.

Although its exact role is unclear, the O-GlcNAc axis has been shown to play a role in synaptic plasticity. A recent study demonstrated that pharmacologically elevating or reducing protein O-GlcNAcylation levels failed to alter basal hippocampal synaptic firing at the Schaffer collaterals in slices (Tallent et al., 2009). However, in vivo elevation of O-GlcNAc enhanced long term potentiation (LTP) and inhibition of O-GlcNAc resulting in a reciprocal affect (Tallent et al., 2009). This phenomena was attributed to increases in phosphorylation of SynapsinI/II due to O-GlcNAc elevation. Another study observed similar results with LTP and reveal that inhibition of OGT promoted LTP through translocation of AMPA receptor subunits (GluR1, and GluR2) to the plasma membrane (Kanno et al., 2010). Our siRNA knockdown of OGT studies (supplementary Fig. 1) recapitulate these prior

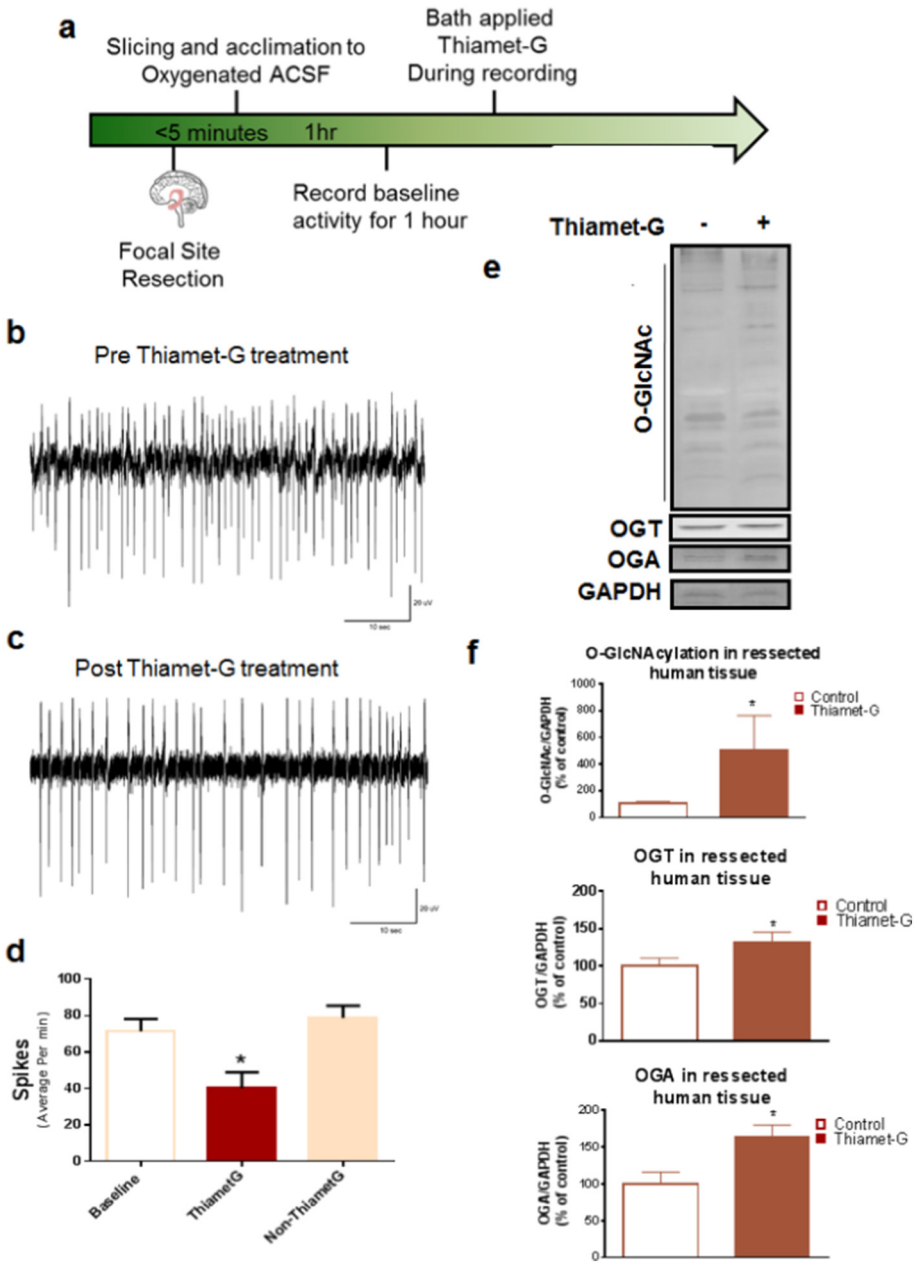

Fig. 6. Thiamet-G bath application on human resected tissue reduced interictal-like activity and increased OGT, and OGA protein expression. (a) Experimental outlined. Samples were taken from patients that had undergone temporal lobectomy. Samples were immediately placed in oxygenated ACSF and allowed to acclimate for 1 h. Baseline recording of activity was taken for 1 h followed by bath application of Thiamet-G. Samples were flash frozen and stored at −80 °C. (b) Representative extracellular recording following Thiamet-G administration (c) Representative extracellular recording following Thiamet-G bath application. (d) Quantification of spiking events from tissue slices at baseline and following Thiamet-G administration. (e) Protein O-GlcNAcylation OGT and OGA representative western blots. (f) Quantification of western blots in *Panel e* where O-GlcNAc, OGT, and OGA were normalized to actin and compared to untreated controls ($n = 4$/group). * denotes $P < .05$. Fisher LSD test. Error bars are SEM.

observations, suggesting that loss of OGT in epilepsy may be facilitating basal synaptic transmission at the synaptic level. Moreover, a recent study indicate that Thiamet-G treatment resulted in AMPA receptor GluA2 O-GlcNAcylation and promoted NMDA receptor and protein kinase C-independent long term depression (LTD) in hippocampal slices (Taylor et al., 2014). Together, these findings present a potential mechanism by which Thiamet-G decreases epileptiform activity observed in our human resected TLE hippocampus.

Our human electrophysiological data reveal decreases in epileptiform activity following Thiamet-G administration indicating that it may be functioning through PTM of proteins altering their structure and function over indirect interactions with ionic channels/receptors. Interestingly, we observed that acute treatment with Thiamet-G did not result in an immediate decrease in seizure activity in our epileptic rodents that underwent EEG recordings (Fig. 3). Instead, our EEG recordings revealed that it was only after three days of Thiamet-G treatment that the drug resulted in decreases in epileptiform brain activity. Collectively, these data suggest that bath application of Thiamet-G onto brain slices compared to in vivo administration has a timed-delay. Thus, Thiamet-G had to first cross the blood brain barrier to inhibit OGA, elevate global protein O-GlcNAcylation, and alter the proteomic landscape that resulted in decreased epileptiform activity.

It has not evaded our attention that although we observed decreased bulk protein O-GlcNAcylation levels in the epileptic hippocampus, this is not necessarily reflective of decreased O-GlcNAc at all individual proteins. In particular, proteomics analysis revealed that SORL-1, a multifunctional endocytic receptor, had increases in O-GlcNAcylation in the epileptic hippocampus. Immunoprecipitations studies revealed that OGA inhibition, which promotes increases in global O-GlcNAcylation, resulted in loss of this PTM at the SORL-1 protein. Much like phosphorylation, O-GlcNAcylation can have structural and functional consequences on proteins that can enhance its overall function/activity or mute it (Wu et al., 1999; Liang et al., 2006). The role of 1980S-OG on SORL-1 is unknown at the moment but given that it was identified in untreated epileptic tissue, it may be perturbing its function in epilepsy to contribute to the hyper excitability observed in this disorder. Furthermore, SORL-1 has a plethora of sites that have been identified to be phosphorylated, and it has been established that there is

extensive crosstalk between phosphorylation and O-GlcNAcylation (Butkinaree et al., 2010; Wang et al., 2008; Wang et al., 2007). One particular study from Wang et al. showed that phosphorylation sites from hundreds of peptides where not actively recycled, but with increases in O-GlcNAcylation it caused major losses of phosphorylation, however increases were observed as well (Wang et al., 2008). Resonating the interplay and competition between phosphoproteome and O-GlcNAc proteome specific kinases such as GSK3β have been demonstrated to increase O-GlcNAcylation of many cytoskeletal and heat shock proteins when GSK3β was inhibited, and at the same time demonstrating decreases in nuclear protein O-GlcNAcylation (Wang et al., 2007). Notably, the bi-directionality of this PTM and interplay with phosphorylation can serve as a biomarker of epilepsy and potentially as a measure of treatment options that result in decreases in epileptiform activity.

O-GlcNAcylation is critical in modulating cellular homeostasis; aberrant O-GlcNAcylation can result in inappropriate protein trafficking, degradation, transcription, translation, and overall function that could lead to cellular death (Pekkurnaz et al., 2014; Xu et al., 2012; Ozcan et al., 2010). Our study suggest that loss of O-GlcNAc homeostasis in epilepsy may affect the neuronal cytoskeleton with loss of O-GlcNAc on Tmod2, as well as protein endocytosis/signaling with SORL1 demonstrating an alternative PTM profile in disease and in treatment. Furthermore, neuronal death is suggested in our T_2 weighted MRI images, where epileptic animals that were administered chronic Thiamet-G treatment in displayed increases in ventricle size and hippocampal atrophy. Tmod2 has been previously described to be altered in Down syndrome, TLE, post-seizures, and post-stroke, but its PTMs in these disorders have not yet been characterized (Yang et al., 2006; Sussman et al., 1994; Sun et al., 2011; Chen et al., 2007). Our study proposes that Tmod2 may be functionally compromised in epilepsy due to its loss of O-GlcNAc at specific residues, and this may also be the case in the other neurological disorders where Tmod2 dysfunction has been implicated (Yang et al., 2006; Sussman et al., 1994; Sun et al., 2011; Chen et al., 2007).

Present TLE medications predominantly target ion channels that are expressed ubiquitously throughout the body, are associated with multiple side effects, and have a 66–75% success rate in controlling seizures with patients. In light of current and previous findings, O-GlcNAcylation provides a promising new therapeutic target in epilepsy or TLE and other chronic seizures disorders (Zachara & Hart, 2006; Hart et al., 2011; Bond & Hanover, 2015). O-GlcNAcylation's immersive role in cellular metabolism, allows it to be regulated by the availability of glucose, amino acids, fatty acids, and nucelotides. Indeed, the O-GlcNAc axis can also be regulated with a variety of other metabolites ranging from glucosamine to diets such as the ketogenic diet, which has been implemented in epilepsy cases (Walgren et al., 2003; Housley et al., 2008; Kang et al., 2008; Lima et al., 2016; Rogovik & Goldman, 2010; de Lima et al., 2014). The ketogenic diet has been demonstrated to aid in epilepsy through disruption of glutametergic signaling, inhibition of glycolysis and activation of ATP dependent potassium channels (Lutas & Yellen, 2013). By favoring a high fat diet over carbohydrates such as in the ketogenic diet, the hexosamine biosynthesis pathway (HBP) production is promoted even with a sparsity of glucose (Cheung & Hart, 2008; Zou et al., 2012; Taylor et al., 2008; Chaveroux et al., 2016). These studies have demonstrated that the upregulation of HBP, which is responsible for UDP-GlcNAc used by OGT, as well as the upregulation of OGT levels provides the combination of substrate availability and enzyme protein levels that lead to global increases in O-GlcNAcylation.

An alternative method to increase O-GlcNAcylation used by Cheung et al., was the use of the FDA approved, economic, and widely used diabetic drug metformin. Metformin stimulates OGT increases via AMP-activated protein kinase (AMPK) signaling, and leads to increase neurofilament H O-GlcNAcylation, a protein that supports neuronal cytoskeletal structures. Our data provide interesting preliminary findings that merit further investigation between beneficial outcome of increased O-GlcNAc with epilepsy and modulating either through several drugs or metabolically through diet. Furthermore, O-GlcNAc signaling has been characterized in numerous pathologies outside of the nervous system (Macauley et al., 2010; Champattanachai et al., 2007; Singh et al., 2015; Lewis & Hanover, 2014).

To date, the study of protein O-GlcNAcylation has been limited to a few neurodegenerative disorders including, Alzheimer's disease (AD), and Parkinson's disease (PD) share overlapping proteomic characteristics with respect to O-GlcNAc and epilepsy. (Gatta et al., 2016; Wani et al., 2017a; Xie et al., 2016; Yuzwa et al., 2014; Narayan et al., 2009; Hung et al., 1980). Altered O-GlcNAcylation levels in the brain was first described in AD studies, showing tauopathies, which is typically hyperphosphorylated in AD, can be O-GlcNAcylated (Yuzwa et al., 2008). By promoting this modification in AD in vivo, it can effectively block tau hyper-phosphorylation, decrease β-amyloid peptide levels and amyloid plaques as well as treat cognitive decline in AD (Yuzwa et al., 2014). Although epilepsy doesn't share the same proteomic hallmarks as AD, AD can be associated with seizures in models of AD as well as in humans (Liu et al., 2018; Hall et al., 2015; Haberman et al., 2017; Born, 2015). While speculative at this point, the phenotypic overlap between AD and epilepsy should be considered when attempting to discover novel proteomic mechanisms to characterize each disorder or novel targets that could be O-GlcNAcylated in each pathology.

The link between PD and protein O-GlcNAcylation was initially through THAP1, a DNA binding protein that regulates cell proliferation via gene transcription and mutations on this gene have lead to DYT6 dystonia (Mazars et al., 2010). THAP1 was found to associate with HCF-1 and OGT in order to promote transcription of cell proliferation factors. This prompted further research to link PD and O-GlcNAc, which lead to studies investigating the role of protein O-GlcNAcylation of α-synuclein, the hallmark protein of PD. Studies showed that indeed α-synuclein can be O-GlcNAcylated and it results in an arrest of its aggregation (Marotta et al., 2015). In modifying α-synuclein with O-GlcNAcylation you also effectively block its degradation (Levine et al., 2017). Furthermore, in postmortem individuals with PD, O-GlcNAcylation is increased, and when this observation is mimiced in primary cortical neurons, the mechanism is associated with increased activation of mTOR (Wani et al., 2017b). The PD field provides insights as to how mTOR O-GlcNAcylation behaves in a neurodegenerative disorder which could provide further insights as to how it could be behaving in epilepsy. In addition, mTOR phosphorylation has been previously assoicated with epilepsy, which highlights the need for further study into the role of O-GlcNAcylated mTOR in epilepsy (Cork et al., 2018; Citraro et al., 2016; Crino, 2016; Duan et al., 2018).

Notably, our findings identified a novel molecular target, OGA, which can be successfully depressed by Thiamet-G in order to promote O-GlcNAcylation levels and decrease the number of seizures and spikes in vivo both in rats and in human tissue. Although chronic inhibition of OGA in epileptic rats did not prevent or reverse ventricular expansion, we observed that Thiamet-G treatment in epileptic animals and humans tissue could be used to reduce seizures and spike frequency. In future studies, it may be of interest to treat these rats with Thiamet-G during earlier stages of epilepsy pathogenesis, or during the onset of status epilepticus to investigate whether Thiamet-G has a better therapeutic effect in delaying or halting epileptogenesis.

In summary, our results suggest a new role for protein O-GlcNAcylation and OGT/OGA mediators in TLE. Homeostatic expression of O-GlcNAcylation appears to be necessary in order to reduce seizures. These findings shed new light on the disorder and warrant further mechanistic studies on novel molecular targets that we have discovered. Considering that protein O-GlcNAcylation is interconnected with broader cellular metabolism, many exciting treatment programs could be employed such as diet to target O-GlcNAcylation's role in epileptic pathophysiology. These therapies would consequently be targeted at the cellular metabolism level in order to regain homeostatic

levels of O-GlcNAcylation.

Supplementary data to this article can be found online at https://doi.org/10.1016/j.nbd.2019.01.001.

Acknowledgments

We would like to thank Drs. Cristin Gavin and Jing Wang of the Evelyn F. McKnight Synaptic Plasticity Core at UAB for technical assistance with electrophysiology experiments. We would like also like to thank Dr. James Mobley for carrying out the mass spectrometry at University of Alabama at Birmingham (UAB) Mass Spectrometry/Proteomics Shared Facility. This work was supported by the Epilepsy Foundation, McNulty Civitan International Scientist Award, and the National Institute of Neurological Disorders and Stroke (NS090250).

References

Al Sufiani, F., Ang, L.C., 2012. Neuropathology of temporal lobe epilepsy. Epilepsy Res. Treatment 2012, 13.
Beissbarth, T., et al., 2004. Statistical modeling of sequencing errors in SAGE libraries. Bioinformatics 20 (Suppl. 1), i31–i39.
Bhatia, V.N., et al., 2009. Software tool for researching annotations of proteins: open-source protein annotation software with data visualization. Anal. Chem. 81 (23), 9819–9823.
Bond, M.R., Hanover, J.A., 2015. A little sugar goes a long way: the cell biology of O-GlcNAc. J. Cell. Biol. 208 (7), 869–880.
Born, H.A., 2015. Seizures in Alzheimer's disease. Neuroscience 286, 251–263.
Bu, G., 2001. The roles of receptor-associated protein (RAP) as a molecular chaperone for members of the LDL receptor family. Int. Rev. Cytol. 209, 79–116.
Butkinaree, C., Park, K., Hart, G.W., 2010. O-linked beta-N-acetylglucosamine (O-GlcNAc): extensive crosstalk with phosphorylation to regulate signaling and transcription in response to nutrients and stress. Biochim. Biophys. Acta. 1800 (2), 96–106.
Cahn, B.R., Polich, J., 2006. Meditation states and traits: EEG, ERP, and neuroimaging studies. Psychol. Bull. 132 (2), 180–211.
Champattanachai, V., Marchase, R.B., Chatham, J.C., 2007. Glucosamine protects neonatal cardiomyocytes from ischemia-reperfusion injury via increased protein-associated O-GlcNAc. Am. J. Physiol. Cell. Physiol. 292 (1), C178–C187.
Chaveroux, C., et al., 2016. Nutrient shortage triggers the hexosamine biosynthetic pathway via the GCN2-ATF4 signalling pathway. Sci. Rep. 6, 27278.
Chen, A., et al., 2007. Upregulation of dihydropyrimidinase-related protein 2, spectrin alpha II chain, heat shock cognate protein 70 pseudogene 1 and tropomodulin 2 after focal cerebral ischemia in rats—a proteomics approach. Neurochem. Int. 50 (7–8), 1078 86.
Cheung, W.D., Hart, G.W., 2008. AMP-activated protein kinase and p38 MAPK Activate O-GlcNAcylation of neuronal proteins during glucose deprivation. J. Biol. Chem. 283 (19), 13009–13020.
Citraro, R., et al., 2016. mTOR pathway inhibition as a new therapeutic strategy in epilepsy and epileptogenesis. Pharmacol. Res. 107, 333–343.
Cole, R.N., Hart, G.W., 2001. Cytosolic O-glycosylation is abundant in nerve terminals. J Neurochem 79 (5), 1080–1089.
Copeland, R.J., G. Han, and G.W. Hart, O-GlcNAcomics–revealing roles of O-GlcNAcylation in disease mechanisms and development of potential diagnostics. Proteom. Clin. Appl., 2013. 7(9–10): p. 597–606.
Cork, G.K., Thompson, J., Slawson, C., 2018. Real talk: the inter-play between the mTOR, AMPK, and hexosamine biosynthetic pathways in cell signaling. Front Endocrinol. (Lausanne) (9), 522.
Coulter, D.A., Steinhauser, C., 2015. Role of astrocytes in epilepsy. Cold Spring Harb. Perspect. Med. 5 (3), a022434.
Crespel, A., et al., 2002. Inflammatory reactions in human medial temporal lobe epilepsy with hippocampal sclerosis. Brain Res. 952 (2), 159–169.
Crino, P.B., 2016. The mTOR signalling cascade: paving new roads to cure neurological disease. Nat. Rev. Neurol. 12 (7), 379–392.
Cunningham, M.O., et al., 2012. Glissandi: transient fast electrocorticographic oscillations of steadily increasing frequency, explained by temporally increasing gap junction conductance. Epilepsia 53 (7), 1205–1214.
Dabbs, K., et al., 2012. Brain structure and aging in chronic temporal lobe epilepsy. Epilepsia 53 (6), 1033–1043.
Duan, W., Chen, Y., Wang, X.R., 2018. MicroRNA155 contributes to the occurrence of epilepsy through the PI3K/Akt/mTOR signaling pathway. Int. J. Mol. Med. 42 (3), 1577–1584.
Ekins, S., et al., 2006. Algorithms for network analysis in systems-ADME/Tox using the MetaCore and MetaDrug platforms. Xenobiotica 36 (10−11), 877–901.
Engel Jr., J., 1996. Surgery for seizures. N Engl J Med 334 (10), 647–652.
Ferrer, I., et al., 2007. Brain protein preservation largely depends on the postmortem storage temperature: implications for study of proteins in Human Neurologic Diseases and Management of Brain Banks: a BrainNet Europe study. J Neuropathol Exp Neurol 66 (1), 35–46.
Fisher, R.S., et al., 1992. High-frequency EEG activity at the start of seizures. J. Clin. Neurophysiol. 9 (3), 441–448.
Fuerst, D., et al., 2003. Hippocampal sclerosis is a progressive disorder: a longitudinal volumetric MRI study. Ann. Neurol. 53 (3), 413–416.
Gass, P., Kiessling, M., Bading, H., 1993. Regionally selective stimulation of mitogen activated protein (MAP) kinase tyrosine phosphorylation after generalized seizures in the rat brain. Neurosci. Lett. 162 (1–2), 39–42.
Gatta, E., et al., 2016. Evidence for an imbalance between tau O-GlcNAcylation and phosphorylation in the hippocampus of a mouse model of Alzheimer's disease. Pharmacol. Res. 105, 186–197.
Golub, T.R., et al., 1999. Molecular classification of cancer: class discovery and class prediction by gene expression monitoring. Science 286 (5439), 531–537.
Haberman, R.P., Koh, M.T., Gallagher, M., 2017. Heightened cortical excitability in aged rodents with memory impairment. Neurobiol. Aging 54, 144–151.
Haddad, T., et al., 2014. Temporal epilepsy seizures monitoring and prediction using cross-correlation and chaos theory. Healthcare Technol. Lett. 1 (1), 45–50.
Hall, A.M., et al., 2015. Tau-dependent Kv4.2 depletion and dendritic hyperexcitability in a mouse model of Alzheimer's disease. J. Neurosci. 35 (15), 6221–6230.
Hart, G.W., et al., 2011. Cross talk between O-GlcNAcylation and phosphorylation: roles in signaling, transcription, and chronic disease. Annu. Rev. Biochem. 80, 825–858.
Hensley, K., et al., 1995. Membrane protein alterations in rodent erythrocytes and synaptosomes due to aging and hyperoxia. Biochim. Biophys. Acta 1270 (2–3), 203–206.
Housley, M.P., et al., 2008. O-GlcNAc regulates FoxO activation in response to glucose. J. Biol. Chem. 283 (24), 16283–16292.
Hung, W.Y., Mold, D.E., Tourian, A., 1980. Huntington's-chorea fibroblasts. Cellular protein glycosylation. Biochem. J. 190 (3), 711–719.
Jackson, D.C., et al., 2011. Ventricular enlargement in new-onset pediatric epilepsies. Epilepsia 52 (12), 2225–2232.
Kang, E.S., et al., 2008. O-GlcNAc modulation at Akt1 Ser473 correlates with apoptosis of murine pancreatic beta cells. Exp. Cell Res. 314 (11−12), 2238–2248.
Kanno, T., et al., 2010. Regulation of AMPA receptor trafficking by O-glycosylation. Neurochem. Res. 35 (5), 782–788.
Keller, A., et al., 2002. Empirical statistical model to estimate the accuracy of peptide identifications made by MS/MS and database search. Anal. Chem. 74 (20), 5383–5392.
Khidekel, N., et al., 2007. Probing the dynamics of O-GlcNAc glycosylation in the brain using quantitative proteomics. Nat. Chem. Biol. 3 (6), 339–348.
Lagerlof, O., Hart, G.W., Huganir, R.L., 2017. O-GlcNAc transferase regulates excitatory synapse maturity. Proc. Natl. Acad. Sci. U S A 114 (7), 1684–1689.
Lagerlof, O., et al., 2016. The nutrient sensor OGT in PVN neurons regulates feeding. Science 351 (6279), 1293–1296.
Levine, P.M., et al., 2017. O-GlcNAc modification inhibits the calpain-mediated cleavage of α-synuclein. Bioorg. Med. Chem. 25 (18), 4977–4982.
Lewis, B.A., Hanover, J.A., 2014. O-GlcNAc and the Epigenetic Regulation of Gene Expression.
Liang, F.C., et al., 2006. Tuning the conformation properties of a peptide by glycosylation and phosphorylation. Biochem. Biophys. Res. Commun. 342 (2), 482–488.
de Lima, P.A., de Brito Sampaio, L.P., Damasceno, N.R.T., 2014. Neurobiochemical mechanisms of a ketogenic diet in refractory epilepsy. Clinics 69 (10), 699–705.
Lima, V.V., et al., 2016. High fat diet increases O-GlcNAc levels in cerebral arteries: a link to vascular dysfunction associated with hyperlipidemia/obesity? Clin. Sci. 130 (11), 871–880 London, England: 1979.
Liu, H., Sadygov, R.G., Yates 3rd, J.R., 2004. A model for random sampling and estimation of relative protein abundance in shotgun proteomics. Anal. Chem. 76 (14), 4193–4201.
Liu, X.Y., et al., 2008. Comparative proteomics and correlated signaling network of rat hippocampus in the pilocarpine model of temporal lobe epilepsy. Proteomics 8 (3), 582–603.
Liu, D., et al., 2018. Brain regional synchronous activity predicts tauopathy in 3xTgAD mice. Neurobiol. Aging 70, 160–169.
Lubin, F.D., et al., 2005. Kainate mediates nuclear factor-kappa B activation in hippocampus via phosphatidylinositol-3 kinase and extracellular signal-regulated protein kinase. Neuroscience 133 (4), 969–981.
Lutas, A., Yellen, G., 2013. The ketogenic diet: metabolic influences on brain excitability and epilepsy. Trends Neurosci. 36 (1), 32–40.
Macauley, M.S., et al., 2010. Elevation of global O-GlcNAc in rodents using a selective O-GlcNAcase inhibitor does not cause insulin resistance or perturb glucohomeostasis. Chem. Biol. 17 (9), 949–958.
Marotta, N.P., et al., 2015. O-GlcNAc modification blocks the aggregation and toxicity of the protein alpha-synuclein associated with Parkinson's disease. Nat. Chem. 7 (11), 913–920.
Mazars, R., et al., 2010. The THAP-Zinc finger protein THAP1 associates with coactivator HCF-1 and O-GlcNAc transferase: A LINK BETWEEN DYT6 AND DYT3 DYSTONIAS. J. Biol. Chem. 285 (18), 13364–13371.
McCullumsmith, R.E., et al., 2014. Postmortem brain: an underutilized substrate for studying severe mental illness. Neuropsychopharmacology 39 (1), 65–87.
Meriaux, C., et al., 2014. Human temporal lobe epilepsy analyses by tissue proteomics. Hippocampus 24 (6), 628–642.
Mielke, K., et al., 1999. Activity and expression of JNK1, p38 and ERK kinases, c-Jun N-terminal phosphorylation, and c-jun promoter binding in the adult rat brain following kainate-induced seizures. Neuroscience 91 (2), 471–483.
Narayan, S., et al., 2009. Evidence for disruption of sphingolipid metabolism in schizophrenia. J. Neurosci. Res. 87 (1), 278–288.
Nateri, A.S., et al., ERK activation causes epilepsy by stimulating NMDA receptor activity. Embo. J., 2007. 26(23): p. 4891–901.
Old, W.M., et al., 2005. Comparison of label-free methods for quantifying human proteins by shotgun proteomics. Mol. Cell Proteomics 4 (10), 1487–1502.

Ozcan, S., Andrali, S.S., Cantrell, J.E., 2010. Modulation of transcription factor function by O-GlcNAc modification. Biochim. Biophys. Acta 1799 (5–6), 353–364.
Pekkurnaz, G., et al., 2014. Glucose regulates mitochondrial motility via Milton modification by O-GlcNAc transferase. Cell 158 (1), 54–68.
Racine, R.J., 1972. Modification of seizure activity by electrical stimulation. I. After-discharge threshold. Electroencephalogr. Clin. Neurophysiol. 32 (3), 269–279.
Rogovik, A.L., Goldman, R.D., 2010. Ketogenic diet for treatment of epilepsy. Canad. Family Phys. 56 (6), 540–542.
Roopun, A.K., et al., A nonsynaptic mechanism underlying interictal discharges in human epileptic neocortex. Proc. Natl. Acad. Sci. U S A, 2010. 107(1): p. 338–43.
Simon, A., et al., 2014. Gap junction networks can generate both ripple-like and fast ripple-like oscillations. Eur. J. Neurosci. 39 (1), 46–60.
Singh, J.P., et al., 2015. O-GlcNAc signaling in cancer metabolism and epigenetics. Cancer Lett. 356 (2), 244–250 Pt A.
Sofroniew, M.V., Vinters, H.V., 2010. Astrocytes: biology and pathology. Acta Neuropathol. 119 (1), 7–35.
Stewart, L.T., et al., 2017. Acute increases in protein O-GlcNAcylation dampen epileptiform activity in hippocampus. J. Neurosci. 37 (34), 8207–8215.
Sun, Y., et al., 2011. A gel-based proteomic method reveals several protein pathway abnormalities in fetal down syndrome brain. J. Proteomics 74 (4), 547–557.
Sussman, M.A., et al., 1994. Neural tropomodulin: developmental expression and effect of seizure activity. Brain Res. Dev. Brain Res. 80 (1–2), 45–53.
Tallent, M.K., et al., 2009. In vivo modulation of O-GlcNAc levels regulates hippocampal synaptic plasticity through interplay with phosphorylation. J. Biol. Chem. 284 (1), 174–181.
Taylor, R.P., et al., 2008. Glucose deprivation stimulates O-GlcNAc modification of proteins through up-regulation of O-linked N-acetylglucosaminyltransferase. J. Biol. Chem. 283 (10), 6050–6057.
Taylor, E.W., et al., 2014. O-GlcNAcylation of AMPA receptor GluA2 is associated with a novel form of long-term depression at hippocampal synapses. J. Neurosci. 34 (1), 10–21.
Thom, D., 1917. Dilatiation of the lateral ventricles as a common brain lesion in epilepsy. H. Nerv. Ment. Dis. 46, 355–358.
Walgren, J.L., et al., 2003. High glucose and insulin promote O-GlcNAc modification of proteins, including alpha-tubulin. Am. J. Physiol. Endocrinol. Metab. 284 (2), E424–E434.
Wang, Z., Gucek, M., Hart, G.W., 2008. Cross-talk between GlcNAcylation and phosphorylation: site-specific phosphorylation dynamics in response to globally elevated O-GlcNAc. Proc. Natl. Acad. Sci. U S A 105 (37), 13793–13798.
Wang, Z., Pandey, A., Hart, G.W., 2007. Dynamic interplay between O-linked N-acetylglucosaminylation and glycogen synthase kinase-3-dependent phosphorylation. Mol. Cell Proteomics 6 (8), 1365–1379.
Wani, W.Y., et al., 2017a. O-GlcNAcylation and neurodegeneration. Brain Res. Bull. 133, 80–87.
Wani, W.Y., et al., 2017b. O-GlcNAc regulation of autophagy and alpha-synuclein homeostasis; implications for Parkinson's disease. Mol. Brain 10 (1), 32.
Weatherly, D.B., et al., 2005. A Heuristic method for assigning a false-discovery rate for protein identifications from Mascot database search results. Mol. Cell Proteomics 4 (6), 762–772.
Webb, W.M., et al., 2017. Dynamic association of epigenetic H3K4me3 and DNA 5hmC marks in the dorsal hippocampus and anterior cingulate cortex following reactivation of a fear memory. Neurobiol. Learn Mem. (142), 66–78 Pt A.
Wieshmann, U.C., et al., 1997. Development of hippocampal atrophy: a serial magnetic resonance imaging study in a patient who developed epilepsy after generalized status epilepticus. Epilepsia 38 (11), 1238–1241.
Worrell, G.A., et al., 2004. High-frequency oscillations and seizure generation in neocortical epilepsy. Brain 127 (7), 1496–1506.
Wu, W.-g., et al., 1999. Structural study on O-glycopeptides: glycosylation-induced conformational changes of O-GlcNAc, O-LacNAc, O-Sialyl-LacNAc, and O-Sialyl-Lewis-X peptides of the mucin domain of MAdCAM-1. J. Am. Chem. Soc. 121 (11), 2409–2417.
Xie, S., et al., 2016. O-GlcNAcylation of protein kinase A catalytic subunits enhances its activity: a mechanism linked to learning and memory deficits in Alzheimer's disease. Aging cell 15 (3), 455–464.
Xu, J., et al., 2012. Regulation of the proteasome by AMPK in endothelial cells: the role of O-GlcNAc transferase (OGT). PLoS ONE 7 (5), e36717.
Xu, W., et al., 2015. Serum profiling by mass spectrometry combined with bioinformatics for the biomarkers discovery in diffuse large B-cell lymphoma. Tumour Biol. 36 (3), 2193–2199.
Yang, J.W., et al., 2006. Aberrant expression of cytoskeleton proteins in hippocampus from patients with mesial temporal lobe epilepsy. Amino Acids 30 (4), 477–493.
Yin, R.H., Yu, J.T., Tan, L., 2015. The role of SORL1 in Alzheimer's Disease. Mol. Neurobiol. 51 (3), 909–918.
Yuzwa, S.A., et al., 2008. A potent mechanism-inspired O-GlcNAcase inhibitor that blocks phosphorylation of tau in vivo. Nat. Chem. Biol. 4 (8), 483–490.
Yuzwa, S.A., et al., 2014. Pharmacological inhibition of O-GlcNAcase (OGA) prevents cognitive decline and amyloid plaque formation in bigenic tau/APP mutant mice. Mol. Neurodegen. 9, 42.
Zachara, N.E., Hart, G.W., 2006. Cell signaling, the essential role of O-GlcNAc!. Biochim. Biophys. Acta 1761 (5–6), 599–617.
Zachara, N.E., et al., 2004. Dynamic O-GlcNAc modification of nucleocytoplasmic proteins in response to stress a survival response of mammalian cells. J. Biol. Chem. 279 (29), 30133–30142.
Zollo, A., et al., 2017. Sortilin-related receptor expression in human neural stem cells derived from Alzheimer's disease patients carrying the APOE epsilon 4 allele. Neural Plast. 2017, 1892612.
Zou, L., et al., 2012. Glucose deprivation-induced increase in protein O-GlcNAcylation in cardiomyocytes is calcium-dependent. J. Biol. Chem. 287 (41), 34419–34431.